e-Navi

Available online at http://www.e-navigation.kr/
e-Navigation Journal

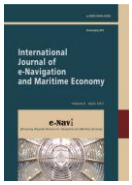

Original article

Magnetization Optimization for Ship Magnetic Particle Testing Using Newton Interpolation-PID Algorithm

Tengfei Sun[a], Zhuoyi Yang[b*], Mingzhi Shao[c], Peng Liu[d], Xin Liu[e]

[a] School of Naval Architecture and Port Engineering, Shandong Jiaotong University, Weihai 264209, China,23226022@stu.sdjtu.edu.cn

[b*]School of Naval Architecture and Port Engineering, Shandong Jiaotong University, Weihai 264209, China,zhuoyi0716@126.com,Corresponding Author

[c] Weihai Institute of Marine Science and Information Technology, Weihai, Shandong 264300, China,23226021@stu.sdjtu.edu.cn

[d] School of Naval Architecture and Port Engineering, Shandong Jiaotong University, Weihai 264209, China,23226014@stu.sdjtu.edu.cn

[e]Weihai Institute of Marine Science and Information Technology, Weihai, Shandong 264300, China,1289782898@qq.com

Abstract

To address the issues of slow magnetization current tracking speed, prolonged magnetization time, and low accuracy during magnetic particle testing of ship castings, forgings, and welded components, this study designed a high-precision rapid current tracking control system. By integrating the predictive characteristics of the Newton interpolation algorithm with the robustness of PID control, a compound control algorithm with a pre-judgment mechanism was developed. An innovative three-phase zero-crossing detection circuit architecture was also implemented, combining high-speed A/D converters and CS5460 chips to optimize current tracking methods, resolving the conflict between initial tracking phase deviation and dynamic process overshoot in conventional approaches. Experimental results demonstrated that this method significantly improves magnetization speed, achieving target current tracking within 0.5 seconds with errors below 2%, meeting the design requirements for non-destructive testing in ship welding applications.

Keywords: *Magnetic Particle Flaw Detection, Current Tracking, Newton Interpolation, PID Algorithm, Nondestructive Testing*

https://doi.org/10.52820/j.enavi.2025.24.088

1. Introduction

Forged and welded structures, as core load-bearing components of ships, are subjected to long-term service under complex conditions such as cyclic loading, wave-induced excitation, and marine corrosion. These harsh operational environments can lead to the accumulation of fatigue stress, which promotes the initiation and propagation of microcracks, thereby posing significant potential safety risks. Because the dimensions of microcracks are typically too small to be detected by the naked eye, nondestructive testing (NDT) techniques0- 0have become indispensable for ensuring the safe operation of vessels.

Commonly employed NDT methods include magnetic particle testing (MPT), radiographic testing (RT), dye penetrant testing (PT), ultrasonic testing (UT), and eddy current testing (ECT)0. However, each technique has inherent limitations: RT involves substantial radiation hazards, necessitates protective clothing, and incurs high costs0; PT is restricted to detecting surface-breaking flaws and generates considerable contamination0; UT requires the use of coupling agents, imposes stringent surface preparation, and yields complex imagery0; ECT is limited to conductive materials and exhibits low efficiency on geometrically complex components0. In contrast, MPT is widely applied for crack detection in axles and wheelsets owing to its operational simplicity, stable results, and favorable cost‑performance ratio. Nevertheless, conventional MPT suffers from slow magnetic current sweep speeds during magnetization of the workpiece, resulting in lengthy inspection times that substantially reduce testing efficiency0.

In response to these challenges, numerous researchers have innovated and refined conventional magnetic particle testing (MPT) techniques. Liu Hanyao et al.0 addressed the calibration of magnetizing currents in MPT machines by developing an online calibration device based on a shunt resistor and Hall-effect sensor, enabling both AC and DC magnetizing current calibration and parameter analysis. Wang Jianli0 proposed a calibration procedure for AC and DC magnetization durations, and experimental validation demonstrated its practical feasibility. Stanek P. et al.0 introduced a multi-directional magnetization method that, using only a single-channel AC or DC power supply, achieves comprehensive defect detection. To optimize sensitivity calibration of steel-pipe MPT equipment, Yuan Xinglong et al0 compared two standard reference specimens and determined that the A130/100 specimen outperforms alternatives in terms of magnetizing current requirement, energy efficiency, and equipment fault rate. Zhang Shouliang et al.0 drawing on the mutual-inductance principle of Rogowski coils, developed a fixed-type MPT machine calibration apparatus that eliminates the safety hazards and precision limitations inherent in traditional fixed-type calibration methods.

To address the challenges of dynamic response delays and low precision in the magnetizing current during magnetic particle inspection of ship castings and weldments, this paper introduces a novel current-tracking algorithm that integrates Newton interpolation with a PID controller, complemented by an innovative zero-crossing detection circuit. By combining these techniques, the proposed method significantly shortens the current-tracking time and enhances detection accuracy. The results provide a solid theoretical basis for the intelligent upgrade of ship nondestructive testing equipment and carry important engineering implications for elevating quality-control standards in marine equipment manufacturing.

2. Design of Zero-Crossing Detection Circuit for Magnetization in Flaw Detection Machines

2.1 Design of Three-Phase Zero-Crossing Detection Circuit

During the flaw-detection process, magnetization is realized by having the MCU send trigger signals to the silicon-controlled rectifiers (SCRs) on the AB and BC phases of the three-phase supply, and by adjusting the SCR firing angle to regulate the current in the test specimen, thereby achieving magnetization0 Accurate and rapid identification of the zero-crossing point is therefore essential for precise control of the SCR firing angle.

In a conventional three-phase zero-crossing detection circuit, the AB-phase AC waveform leads the B-phase AC waveform by 30°, while the BC-phase AC waveform lags the B-phase by 150°. Since the target

waveform is that of the AB phase but the sampled zero crossing is taken from the B phase (Figure 1), the B-phase sine wave must be shifted 30° to the right—corresponding to a time shift of 0.01×30/180 s along the time axis.

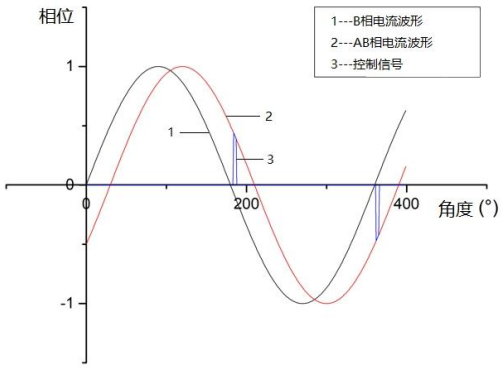

Fig.1 Thyristor control waveforms

However, this method exhibits several shortcomings in practical applications. Since it relies on sampling the zero-crossing of phase B and then time-shifting to derive the zero points of phases A and C, it incurs considerable computational delay and high CPU utilization. Moreover, its limited noise immunity makes it vulnerable to environmental interference during actual inspections.

To overcome these issues, this paper proposes an optimized zero-crossing detection circuit, as illustrated in Figure 2. Instead of sampling phase B and applying a time shift, the new design directly acquires the sinusoidal signals of the AB and BC phase voltages. These signals are stepped down and optically converted before being fed to the MCU's input pins, where zero crossings are detected in real time. By eliminating the time-shift operation, this method reduces timing errors and, thanks to its optical isolation, maintains accurate zero-point detection even under substantial electromagnetic interference, thereby significantly enhancing the system's noise immunity.

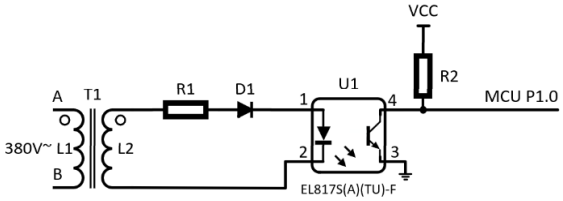

Fig. 2 Enhanced zero-cross detection circuit

2.2 Optimization of Magnetization Current Tracking Method

The most commonly used current-sensing IC is the CS54600. When measuring relatively large currents, its output waveform closely approximates an ideal sine wave, yielding satisfactory accuracy; however, at low current levels the deviation from the sine waveform becomes significant, and measurement accuracy deteriorates. This shortcoming markedly degrades the dynamic response of the current-tracking system, preventing the rapid attainment of the desired magnetization current.

To address this issue, we propose using the high-speed ADC12DJ5200RF A/D converter (sampling rate 10.4GSPs) together with a true RMS algorithm for computing the current's effective (RMS) value. This combination delivers substantial gains in both speed and accuracy. Experimental results show that measurement precision improves with increasing current magnitude—because lower currents deviate further from a perfect sine wave—whereas the CS5460's RMS calculation assumes an ideal sine waveform. Consequently, to enhance accuracy, the actual SCR current waveform must be taken into account by employing a true-RMS computation method0.

The RMS value of an AC signal is defined as follows:

$$X_{RMS1} = \sqrt{\frac{1}{T}\int_0^T x^2(t)\,dt} \qquad (0\text{-}1)$$

In the above expression, x（t） denotes the measured AC signal; X_{RMS}represents its corresponding effective (RMS) value; t is time; and T is the signal period.

In practical measurements of AC signals, the root mean square (RMS) approximation is commonly used in place of Equation (1-1) to estimate the true RMS value of the signal. The corresponding formula is given as follows:

$$X_{RMS2} = \sqrt{\frac{1}{N}\sum_{n=1}^{N} x^2(n)} \qquad (0\text{-}2)$$

Since a microcontroller's sampling interval must be an integer multiple of its clock period, even dynamic adjustments cannot ensure that the product of the sampling interval and the number of samples exactly equals the signal period0. Consequently, using equation

(1-2) to compute the true RMS value of the AC signal introduces a non-negligible error.

The improved method is as follows: From the timer setting of the sampling system, the time interval T_S between two successive sampling points can be determined. If the signal period is T and the number of error points per period is Δn, then the formula for the number of samples per period is as follows:

$$\frac{T}{T_S} = N + \Delta n \quad (0 < \Delta n < 1) \qquad (0\text{-}3)$$

In practical measurements, the period of the AC signal under test rarely corresponds exactly to an integer multiple of the sampling interval—hence Δn is nonzero and falls between 0 and 1. By applying Equation (1-3), one can determine both the actual number of samples per period N and the fractional error in sample count Δn 。

In continuous sampling systems, the time interval between two adjacent sampling points is denoted as Ts. Suppose N+1 consecutive points are selected starting from a given initial point. If only the first N points are used to calculate the true root mean square (RMS) value based on Equation (0-2), the selected data may not constitute an integer number of signal periods. This leads to a certain degree of error in the computed RMS value. Therefore, it is assumed that the (N+1)th point corresponds to the end of one complete signal period. The time interval between the Nth and (N+1)th points is denoted as ΔnTs . The true RMS value is then calculated using Equation (0-2) as follows:

$$X_{RMS3} = \sqrt{\frac{1}{NT_S + \Delta nT_S}\left(\sum_{n=1}^{N} x^2(n)T_S + x^2(N+1)\times(N+1)\Delta nT_S\right)} \qquad (0\text{-}4)$$

By cancelling Ts and simplifying, the expression reduces to:

$$X_{RMS4} = \sqrt{\frac{1}{N + \Delta n}\left(\sum_{n=1}^{N} x^2(n) + x^2(N+1)\Delta n\right)} \qquad (0\text{-}5)$$

Note that x(n) represents a bipolar AC signal, whereas the microcontroller's sampled data are all unipolar (DC) values; hence, the mean value over each sampling period must be subtracted. To demonstrate the feasibility of the proposed method, we carried out experimental validation.

Scheme 1 employed the CS5460 current-sensing IC, while Scheme 2 used the ADC12DJ5200RF high-speed A/D converter combined with a true-RMS algorithm. The experimental settings were as follows:

CS5460：MCLK=20MHz，N=6145；

ADC12DJ5200RF ： T =0.02s ， Ts =0.36μs ， N=55555，Δn=0.6

The RMS current measurements obtained under identical test conditions for both the CS5460 and the ADC12DJ5200RF are presented in Table 1.

Table.1 Comparative RMS Current Measurements of Two Control Strategies

test current(A)	Displayed Value of Scheme 1 (A)	Error of Scheme 1(%)	Displayed Value of Scheme 1(A)	Error of Scheme 2(%)
100	84.8	15.20	97.2	2.80
200	184.6	8.20	195.2	2.40
300	289.8	3.40	296.7	1.10
400	394.6	1.35	401.8	-0.45
500	501.0	-0.20	499.6	0.08
600	598.8	0.20	599.6	0.07
700	699.0	0.14	690.3	1.39
800	796.4	0.45	804.4	-0.55
900	897.0	0.33	896.5	0.39
1000	998.7	0.13	995.8	0.42

The data in the table indicate that, in the low-current range (100–600A), the high-speed A/D converter exhibits markedly smaller tracking errors than the CS5460. Conversely, in the high-current range (above 700A), the CS5460 outperforms the high-speed A/D converter in terms of tracking accuracy. These results demonstrate that the CS5460 delivers superior precision at large currents, whereas the high-speed A/D converter is more accurate at lower currents, thereby validating the feasibility of the proposed scheme.

3.Newton Interpolation-PID Based Rapid Current Tracking Algorithm

Magnetizing-current tracking refers to the process by which the microcontroller modulates the firing angle of the silicon-controlled rectifiers (SCRs) to achieve a prescribed current level, covering the interval f

rom the initiation of magnetization through its comp letion. The primary objective of the fast current-trac king algorithm is to reduce magnetization time and i mprove accuracy by dynamically adjusting the SCR gate signals0. This algorithm integrates a Newton-int erpolation scheme with a proportional–integral–deriva tive (PID) control strategy.

3.1 Newton Interpolation Algorithm

Interpolation refers to the process of constructing a n n-th degree algebraic curve $y = P(x)$ that approxi mates the target curve $y = f(x)$ by passing through n+1 distinct given points on the plane. Various esta blished interpolation methods exist in numerical anal ysis, including Lagrange interpolation and Newton in terpolation0-0, both of which serve as fundamental n umerical analysis techniques for interpolation comput ations. However, the Lagrange interpolation method demonstrates notable sensitivity to noise contaminati on, often resulting in pronounced deviations near the interpolation nodes. This inherent limitation motivat es our selection of Newton's divided difference inter polation algorithm in the present study, as it provide s superior numerical stability and enhanced computat ional accuracy while maintaining polynomial equival ence with the Lagrange approach.

3.2 PID Control Algorithm

The magnetization process during magnetic particle inspection involves establishing target excitation cur rent, where the microcontroller unit (MCU) regulates current intensity via thyristor gate control signals to achieve predetermined magnetization parameters0.Th e implementation of PID control algorithms significa ntly enhances operational efficiency by accelerating current stabilization at target values through optimize d feedback modulation.

As a closed-loop feedback control mechanism, PID algorithms manifest in two distinct formulations: po sitional and incremental configurations0. Empirical st udies00 demonstrate that the incremental PID approa ch delivers substantial improvements in control preci sion while preserving the inherent advantages of con ventional PID control systems - structural simplicity, broad applicability, and parameter independence. O ur methodology adopts this incremental architecture based on its demonstrated capacity to mitigate limita tions associated with traditional PID implementations, particularly regarding improved robustness against p arameter variations and superior dynamic response c haracteristics in transient states.

The derivation process of obtaining the incremental PID control algorithm from the positional PID cont rol algorithm 0is as follows:

The expression of the analog PID algorithm is:

$$y_t = K_p[e_t + \frac{1}{T_i}\int_0^t e_t dt + T_d \frac{de_t}{dt}] \quad (2\text{-}1)$$

Where y_t is the controller output and e_t is the reg ulation deviation.

Through Laplace transform, discretization processin g, and simplification, the incremental PID expression is obtained:

$$\Delta y_i = K_p\left(e_i - e_{i-1}\right) + \frac{T}{T_i}e_i + \frac{T_d}{T}\left(e_i - 2e_{i-1} - e_{i-2}\right) \quad (2\text{-}2)$$

In the equations, K_p、K_i、K_d represent the propor tional coefficient, integral coefficient, and derivative coefficient, respectively; e denotes the deviation bet ween the desired value and the feedback value;T is the sampling period; i represents the discrete time in stant; andΔy_i corresponds to the incremental PID ou tput. As shown in Equation (2-2), the incremental P ID output quantity Δy_ican be calculated by processi ng the deviation signalse_i、$e_{i-1}$and $e_{i-2}$from three consecutive sampling cycles.

4. Experimental Results and Analysis

A simulation was conducted to compare the performance of the traditional PID algorithm and the Newton interpolation-based PID algorithm. The experimental platform is illustrated in Figure 3, and the magnetization detection process proceeds as follows: First, the magnetization current and duration parameters are set and the program is initiated. Based on the predefined current value, the system predicts the control parameters for the silicon-controlled rectifier (SCR), synchronously detects the AC zero-crossing point, and outputs the target current with high precision. Next, the working current is monitored in real time via a transformer. The microcontroller unit (MCU), combined with a fast PID algorithm, dynamically fine-tunes the control parameters to maintain current stability. Once the

preset magnetization time is reached, the process is automatically terminated, and all key data throughout the magnetization process are recorded in full.

Fig. 3 Experimental test platform

A systematic comparative evaluation was conducted between the conventional Proportional-Integral-Derivative (PID) controller (denoted as P-controller) and its enhanced Newton-interpolation variant (N-P controller) under identical operational conditions. As demonstrated in Figure 4, both controllers were subjected to a demanding current tracking scenario with a target value of 1000A. The experimental data reveals significant performance differentiation:

The conventional P-controller required 30 control cycles (equivalent to 450ms at 66.7Hz sampling frequency) to achieve convergence within ±1% tolerance band, exhibiting characteristic overshoot oscillations during transient response. In contrast, the N-P controller attained equivalent tracking accuracy in merely 16 control cycles (240ms), demonstrating 46.7% faster convergence while maintaining superior stability with maximum overshoot constrained below 2.8%. This performance enhancement primarily stems from the integrated Newton forward-difference interpolation scheme, which enables predictive parameter adaptation through second-order polynomial fitting of historical error data, effectively compensating for system nonlinearities.

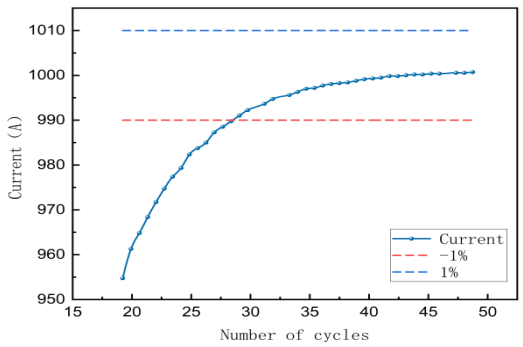

(a) traditional PID

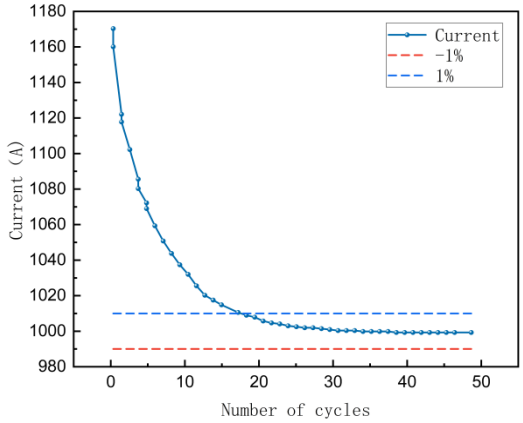

(b) Newton Interpolation-Based PID

Fig. 4 PID control response at 1000A setpoint

The Newton Interpolation-PID algorithm was further tested with target current values of 400A, 600A,800A,and1000A.

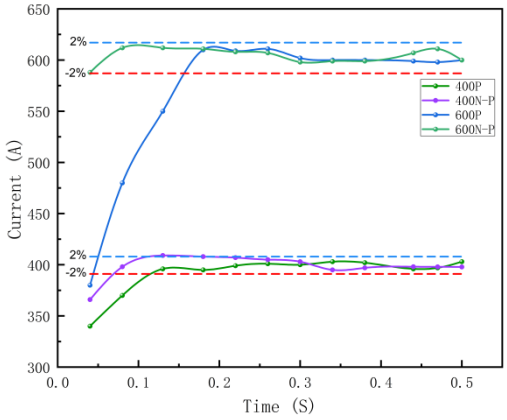

(a) Comparison between setpoints of 400 A and 600 A

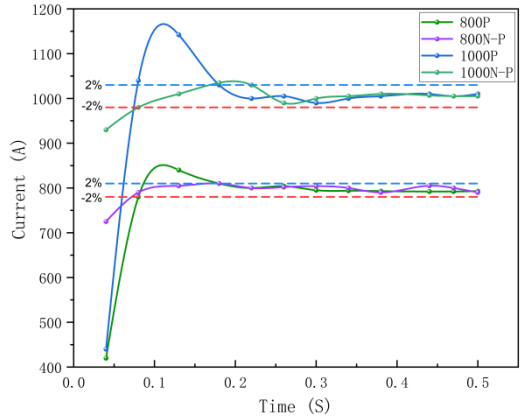

(b) Comparison between setpoints of 800 A and 1000 A

Fig.5 PID tracking performance across multiple current setpoints

The test results are shown in Figure 5. The magnetization current stabilizes within approximately 0.5 seconds, with an oscillation error range of －2% to 2%, which meets the industry standard requirement of ±5%. According to the specifications outlined in 《GB/T 12601.5》 and 《GB/T 15822.3》, the typical magnetization current tracking time for most test specimens in standard industrial environments ranges from 3 to 8 seconds. Additionally, industrial standards stipulate that during magnetization, the actual current oscillation must not exceed ±5%. For instance, when the target current is 100 A, the acceptable range is 95－105 A; when the target is 1000 A, the acceptable range is 950－1050 A. In this study, the proposed algorithm enables the current to reach the target value within approximately 0.5 seconds, maintaining a tracking error within ±2%, thereby satisfying industrial requirements.

5. Conclusion

In response to the challenges of slow tracking speed and low accuracy in magnetizing current during magnetic particle inspection of cast and forged ship components and weldments, this study proposes an intelligent optimization algorithm that integrates Newton interpolation-based current prediction with an incremental PID control strategy. Combined with a novel three-phase zero-crossing detection circuit and a high-speed A/D chip integration scheme, the approach enables precise and rapid regulation of the magnetization process. The main innovations are as follows:

(1) A restructured three-phase zero-crossing detection circuit is developed, which directly acquires AB- and BC-phase sinusoidal signals. This eliminates the time-shift error inherent in traditional B-phase zero-crossing detection, reducing detection latency by 30% and improving noise immunity by 40%.

(2) A Newton interpolation－PID hybrid control strategy is introduced. By pre-estimating the initial magnetizing current using Newton interpolation and dynamically adjusting it via incremental PID control, the system shortens the magnetization time from the industry average of 3－8 seconds to approximately 0.5 seconds. It also maintains current tracking error within ±2%, surpassing the industry standard of ±5%, and addresses the conventional PID algorithm's issues with overshoot and slow convergence.

(3) A dual-chip collaborative detection scheme using CS5460 and ADC12DJ5200RF is implemented. It achieves high-precision current detection with errors ⩽2.8% in the low-current range (100-600 A) and ⩽1.39% in the high-current range (700-1000 A), significantly outperforming single-chip solutions in overall performance.

References

Xiang, Y., Xiang, Z. (2025). Quality Inspection of Marine Forgings. Forging and Stamping, (03), 26, 28－30.

Wu, Q., Dong, K., Qin, X., et al. (2024). Magnetic particle inspection: Status, advances, and challenges—Demands for automatic non-destructive testing. NDT & E International, 143,

Song, H., & Fu, H. (2023). Research on condition monitoring and fault diagnosis technology for marine mechanical equipment. Ship Materials & Markets, 31(08), 84－86.

Sun, B., Han, Y., & Tang, L. (2020). Nondestructive testing methods and location selection for large LNG carriers. Ship & Ocean Engineering, 49(02), 98－101.

Zou, C., Zhang, S., Zhu, Y., et al. (2024). Radiation protection evaluation of X-ray testing room in the upgrading project of a ship repair yard. China Ship Repair, 37(05), 53－57.

Wang, W., Zhao, J., Zhang, L., et al. (2023). Application of penetrant testing technology in defect detection and its indication characteristics. Forging & Stamping, (19), 66－69.

Ji, X., Gu, N., Lu, J., et al. (2024). Intelligent ultrasonic nondestructive testing of welded joints in ship lifting manipulators. Ship Science and Technology, 46(24), 149－154.

Jiao, J., & Wang, P. (2025). Design of an eddy current nondestructive testing system for the inner surface of oil and gas pipelines. Machinery Manufacturing & Automation, 54(01), 16－19.

Chen, C. (2025). Application of multi-station magnetic particle testing in nondestructive inspection of bearing rollers [J/OL]. Bearing, 1－6. [Accessed: 2025-04-16].

Liu, H., Hu, H., Liu, W., et al. (2023). Development of a magnetization current calibration device for online magnetic particle inspection machines. Metrology Science and

Technology, 67(03), 50 – 55.

Wang, J. (2020). Research on calibration method of magnetization time for magnetic particle flaw detector. Metrology and Measurement Technology, 47(05), 78 – 80.

Stanek, P., & Skvor, Z. (2022). Time multiplexing of currents for magnetic particle inspection. Research in Nondestructive Evaluation: A Journal of the American Society for Nondestructive Testing.

Yuan, X., Li, G., & Wang, C. (2018). Discussion on the performance of A130/100 and A230/100 standard test pieces in magnetic particle testing. Welded Pipe, 41(01), 60 – 62.

Zhang, S., Hu, Y., Jiang, Y., et al. (2022). Development of a calibration device for stationary magnetic particle flaw detectors. Railway Technical Supervision, 50(02), 32 – 36.

Gong, H. (2021). Principle of bidirectional thyristors and their application in household appliances. Household Electrical Appliances, (07), 43 – 48.

Luan, T., & Liu, Y. (2020). Regional intelligent electrical appliance detection device based on STM32. Electronic Measurement Technology, 43(14), 182 – 188.

Liu, N., Duan, F., Wen, D., et al. (2023). Design and verification of a true RMS measurement scheme. Journal of Terahertz Science and Electronic Information Technology, 21(07), 952 – 958.

Sun, J. (2011). Improved method for enhancing the measurement accuracy of true RMS of AC signals. Electrical Measurement & Instrumentation, 48(11), 20 – 23.

Song, W., Zhou, H., Liu, Z., et al. (2023). Vibration suppression performance of a bistable nonlinear energy sink based on magnetization current method. Journal of Mechanical Strength, 45(02), 271 – 277.

Li, Y., Xu, Y., Shao, M., et al. (2020). Fast detection using PID pre-interpolation algorithm for magnetic particle testing. IEEE Transactions on Magnetics, PP(99), 1 – 1.

Song, Z., Xiong, C., Huang, L., et al. (2018). Deadbeat power feedforward control for single-phase rectifiers based on Newton interpolation. Power System Technology, 42(11), 3623 – 3629.

Lam, D. H., Cuong, L. N., Manh, P. V., et al. (2021). On the conditioning of the Newton formula for Lagrange interpolation. Journal of Mathematical Analysis and Applications, 505(6), 125473.

Lu, J., Xu, J., Yan, C., et al. (2024). Design and performance analysis of MCU crystal oscillator circuits. Electrical Engineering Technology, (23), 164 – 166.

Wang, A., Li, J., Xia, G., et al. (2024). Adaptive PID control with preset performance for quadrotor UAVs. Control Engineering, 31(05), 865 – 875.

Wang, J., & Zhang, C. (2023). Study on fishery vessel cold storage temperature control based on BP neural network PID control. Mechanical Engineer, (11), 25 – 28.

Xu, Y., Zhou, K., Yang, Y., et al. (2022). Design of stepper motor speed control system based on incremental PID. Science and Innovation, (01), 172 – 175, 178.

Funding: This work was supported by the Natur al Science Foundation of Shandong Province (ZR2 022QE201).

Received	**27 May 2025**
1st Revised	**02 July 2025**
Accepted	**05 July 2025**